19th Brazilian Congress of Thermal Sciences and Engineering
November 06th-10th, 2022, Bento Gonçalves - RS - Brazil

ENC-2022-0578
A NUMERICAL STUDY OF NATURAL CONVECTIVE HEAT TRANSFER FROM A HORIZONTAL TWO-DIMENSIONAL TWO-SIDED PLATE HAVING ONE OR TWO ADIABATIC SECTIONS

Anelize Terroni Teixeira
Santiago del Rio Oliveira
Department of Mechanical Engineering, São Paulo State University, 14-01 Engenheiro Luiz Edmundo Carrijo Coube Avenue, Bauru, SP, 17033-360, Brazil
anelize.teixeira@unesp.br
santiago.oliveira@unesp.br

Abstract. *This study was carried out with the aim of examining the behavior of the presence of adiabatic sections in a flat plate subjected to conditions of natural convective heat transfer, evaluating how the position and size of these adiabatic sections can interfere with natural convective heat transfer rate. To verify this effect, numerical analysis was used by simulating the mathematical model in CFD using ANSYS FLUENT©. The conditions used in the plate for the problem physical modeling were a horizontal, two-dimensional isothermal plate, allowing heat transfer on both plate sides. For the numerical simulation to be possible, it was also necessary to set up some dimensional plate parameters, as well as the plate and air properties. The first cycle of simulations was performed considering the plate divided into 3 equal-sized sections in which the middle section was made up of the adiabatic region. The second cycle of simulations was performed considering the plate was divided into 5 sections of the same size where the second and fourth sections were composed of the adiabatic regions. Both cases were simulated considering a symmetric mean flow concerning the central plate plane, using the* $k-\varepsilon$ *turbulence model with the total account of buoyancy force effects. The results were obtained in terms of comparison between the mean Nusselt number and the Rayleigh number as well as the comparison between the mean heat transfer rates with and without the adiabatic sections. In these simulations, the Prandtl number was considered constant for air.*

Keywords: *Adiabatic sections, Natural convective heat transfer, CFD.*

1. INTRODUCTION

The study of convective heat transfer aims to analyze how heat is transferred between a fluid and an adjacent surface or between fluids, so that, according to (Jiji, 2006), there are three crucial factors for a complete convection heat transfer analysis, being the fluid movement understanding, the nature of flowing fluid and finally, the adjacent surface geometry. Knowing the characteristics of these three factors, it is then possible to obtain the fluid temperature distribution along the surface. In the heat transfer analysis by natural convection, the Grashof number provides the ratio between the buoyant force and the viscous force acting on the fluid, indicating whether the flow occurs in a laminar or turbulent regime. The Grashof number can be replaced by the Rayleigh number in certain analyses, where the Rayleigh number is the product of the Grashof number and the Prandtl number, representing the ratio between the thermal diffusivity and buoyancy forces by the momentum, according to (Çengel and Ghajar, 2009).

Conforming to (Hærvig and Sørensen, 2020), heat transfer by natural convection is highly reliable and cost-effective since it does not require an external source to generate the fluid movement. Regarding natural convection in flat plates, several studies have been developed to evaluate its behavior, as is the case of the works by (Yu and Lin, 1993), (Kitamura and Kimura, 1995), (Laein et al., 2016), (Nazar et al., 2006), (SV et al., 2021), (Samanta and Guha, 2014) and (Guha et al., 2019). There are studies carried out with the aim of evaluating free convection on flat walls in fins, where the surfaces are located parallel to each other, as in the case of studies by (Tari and Mehrtash, 2013) and (Nada, 2007). However, few studies have been carried out to analyze adjacent surfaces, which is a focus of this study. Optimizing an existing process is always a good practice aimed at saving energy and inputs. One way to optimize heat transfer by natural convection is to use surfaces with waves to increase the heat transfer rate, as in the case of studies by (Narayana and Sibanda, 2010) and (Fayz-Al-Asad et al., 2021).

CFD (Computational fluid dynamics) analysis emerged in the 1960s from the aeronautical industry with the premise of performing the analysis of mass flow and heat transfer associated with chemical reactions through to computer simulations. According to (Versteeg and Malalasekera, 2007) the CFD analysis is performed in 3 steps, which are pre-process, solver, and post-process. In pre-process, the flow inputs are inserted, the geometry to be studied and the fluid properties are defined, as well as the boundary conditions specified. In solver, the governing equations of the flow and the fluid are solved iteratively through the discretization process. In the post process, the results obtained through the simulation are represented graphically. Therefore, CFD tools help a lot in the analysis of heat transfer studies, as can be seen in the studies by (Dogan et al., 2014), (Liu et al., 2021), and (Adhikari et al., 2020).

This article aims to perform a numerical analysis of the heat transfer by natural convection in a flat horizontal plate with one or two adiabatic surfaces of the same size distributed along its width, where there is heat transfer on both the upper and lower surfaces (being both heated at the same temperature), analyzing the problem in a two-dimensional way.

2. PHYSICAL MODELING

According to (Incropera and DeWitt, 2008) the Grashof number Gr_L for a plate of width L is given by:

$$\mathrm{Gr}_L = \frac{g\beta(T_S - T_\infty)L^3}{\nu^2} \tag{1}$$

where g is the gravity acceleration in [m/s²], β is the bulk coefficient of expansion [1/K], T_S is the surface temperature [K], T_∞ is the fluid temperature [K], L is the plate width [m] and ν is the kinematic viscosity of the fluid [m²/s].

As the Rayleigh number is the Grashof number and the Prandtl number (ν/α) product, (Incropera and DeWitt, 2008) show the Rayleigh number (Ra_L) of the plate as being:

$$\mathrm{Ra}_L = \frac{g\beta(T_S - T_\infty)L^3}{\nu\alpha} \tag{2}$$

where α is the fluid thermal diffusivity of the fluid [m²/s].

The mean Nusselt number for the plate $\overline{\mathrm{Nu}_L}$ according to (Incropera and DeWitt, 2008) is:

$$\overline{\mathrm{Nu}_L} = \frac{\bar{h}L}{k} \tag{3}$$

where $\bar{h}$ is the heat transfer coefficient [W/(m².K)] and k is the thermal conductivity of the fluid [W/(m.K)]. The heat transfer coefficient is given by:

$$\bar{h} = \frac{q_{(\text{bottom/top})}}{A(T_S - T_\infty)} \tag{4}$$

where A is the plate area in contact with the fluid [m²] and $q_{(\text{bottom/top})}$ is the convection heat transfer rate [W].

Substituting Eq. (4) in Eq. (3) we obtain the mean Nusselt number for analysis of this study evaluating both sides of the plate (bottom and top), as follows:

$$\overline{\mathrm{Nu}_{L\,(\text{bottom/top})}} = \frac{q_{(\text{bottom/top})}L}{kA(T_S - T_\infty)} \tag{5}$$

where $\overline{\mathrm{Nu}_{L\,(\text{bottom/top})}}$ is the mean Nusselt number evaluated on the bottom and on the top of the heated plate surface.

The dimensionless width W_i of the adiabatic sections is defined by the following expression:

$$W_i = \frac{w_i}{L} \tag{6}$$

3. SOLUTION PROCEDURE

3.1 Model and Constants

The numerical results were obtained using the ANSYS FLUENT© software for CFD simulations through the $k-\varepsilon$ standard turbulence model so that the constants used to solve the viscous dissipation equation (ε) and the turbulent kinetic energy equation k was the empirical constants default, conform (Versteeg and Malalasekera, 2007), where C_{μ}=0.09, $C_{1\varepsilon}$ = 1.44, $C_{2\varepsilon}$ = 1.92, σ_k = 1.0 and σ_ε = 1.3 , with the energy Prandtl Number and wall Prandtl number being equal to 0.85. The fluid used in this study was air with 1.225 [kg/m³] for density varying according to the Boussinesq hypothesis and with constant properties being specific heat C_{p_air} = 1006.43 [J/(kg.K)], thermal conductivity k_{air} = 0,0242 [W/(m.K)], dynamic viscosity μ_{air} = $1.7894.10^{-5}$ [kg/(m.s)] and thermal expansion coefficient β_{air} = 0,0033[1/K]. For the plate material, was considered aluminum with the following constant properties: Density ρ_{al} = 2719 [kg/m³], specific heat C_{p_al} = 871,0 [J/(kg.K)], thermal conductivity k_{al} = 202,4 [W/(m.K)]. To configure the spatial discretization was used the First Order Upwind for turbulent kinetic energy, turbulent dissipation rate, momentum, and energy. For the gradient spatial discretization was used the Green-Gauss Cell Based.

3.2 Plate Configuration

The conditions used for the plate in the physical modeling of the problem were a horizontal, two-dimensional isothermal plate, allowing heat transfer on both sides of the plate, these conditions can be seen in Fig. 1 for a generic dimension. In this study, both geometry and the computational domain were considered two-dimensional. For the numerical simulation to be possible, it was also necessary to set up some dimensional parameters of the plate, as well as the properties of the plate and the air. The first cycle of simulations was performed considering the surface temperature of the plate to be 310 K while the ambient air temperature was 290 K, the width and depth of the plate were considered 1 m, and it was divided into 3 equal-sized sections in which the middle section was made up of the adiabatic region. The second simulation cycle was performed considering the same temperatures for the plate and the air as well as the width and depth of the plate, however, the width of the plate was divided into 5 sections of the same size so that the second and fourth sections were adiabatic regions. The plate with the three-section and five-section configurations can be seen in Fig. 2 for a generic dimension (width and depth).

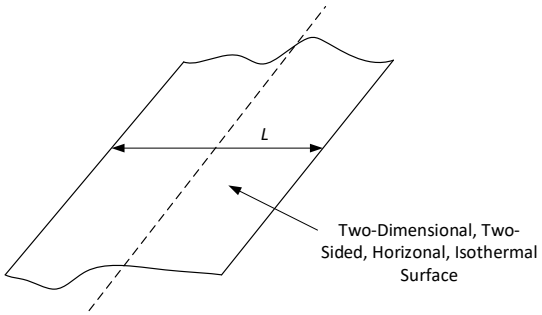

Figure 1. Basic situation being considered, i.e., a horizontal, two-dimensional, thin flat plate with no adiabatic section.

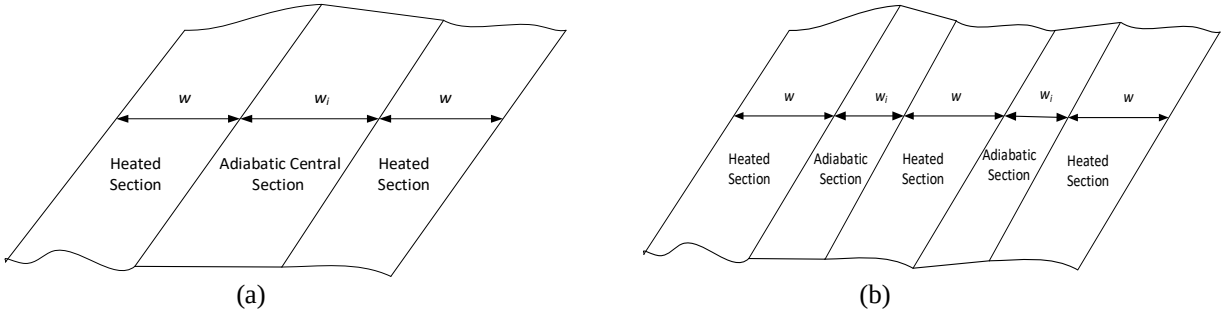

Figure 2. Horizontal, two-dimensional, thin flat plate with (a) one center adiabatic section and (b) two symmetrical adiabatic sections.

Finishing the problem modeling, it was considered that the average flow was constant in all simulations, it was also considered that the fluid had constant properties except for its density which varying according to temperature. For all simulations, the Prandtl number for air was assumed to be 0.74. Since the focus of this study is the heat transfer rate by

natural convection, radiation heat transfer was not considered. Verification of the model convergence criteria was performed. The results were obtained in terms of an average heat transfer rate over the bottom and top surfaces.

4. RESULTS AND DISCUSSION

The numerical results were obtained for the models with one and two adiabatic sections with Rayleigh number varying between 10^9 to 10^{12}. The mean Nusselt number for each case was obtained to the variation of the Rayleigh number, where the simulations performed the heat transfer heat calculus for the plate regions bottom and top. The mean Nusselt number for the bottom and the top was obtained through the Eq. (5), where the heat transfer area was calculated with the width and depth disregarding the adiabatic section area. Gravity was calculated by the Eq. (2), once all parameters are known, with exception of gravity.

In furtherance to compare and validate the results obtained for the adiabatic sections, simulations were performed for Rayleigh number varying between 10^9 to 10^{12}, using the same model and constants, presented in Section 3.1, for a horizontal, two-dimensional isothermal plate, allowing heat transfer on both sides of the plate (bottom and top), with the same dimension and temperature settings in Section 3.2, but without adiabatic sections.

The CFD simulations were performed using a computer with an Intel Core i7-10750H processor and Nvidia GTX 1050 graphic card with 4G DDR6. 32 CFD simulations were performed for both cases, 16 for an adiabatic section and 16 for two adiabatic sections, in a total of 91916 iterations which required 60,18 hours of computational time.

For only one adiabatic section, the simulations were realized for the width W_i of the adiabatic sections ranging from 0.1, 0.2, 0.4, and 0.75 m. These results can be seen in Fig. 4 and 5. The Tab. 1 contains these results in terms of Nusselt number and heat transfer rate for the top and bottom regions for each respective Rayleigh number.

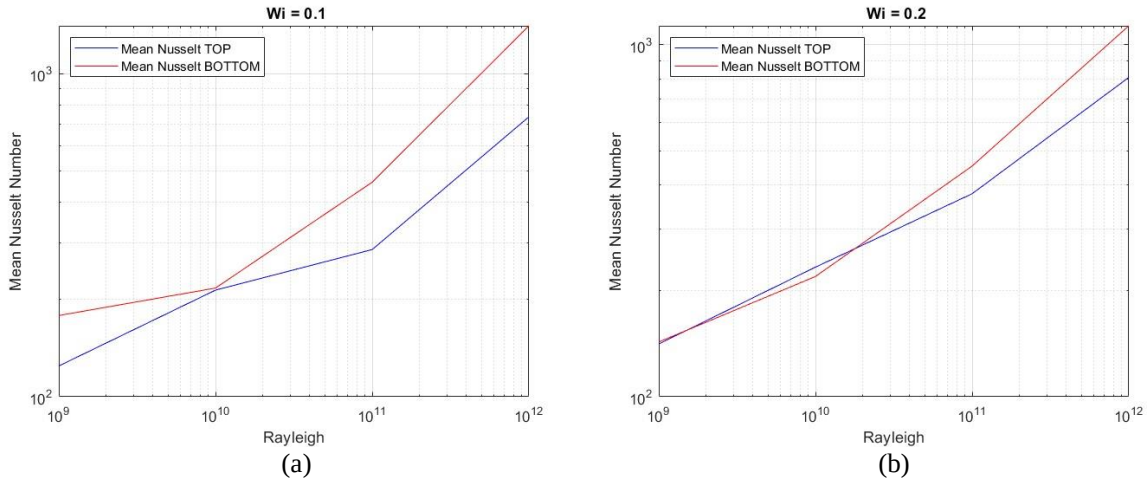

Figure 4. Variation of mean top and mean bottom Nusselt number with Rayleigh number for the case where (a) W_i = 0.1 and (b) W_i = 0.2.

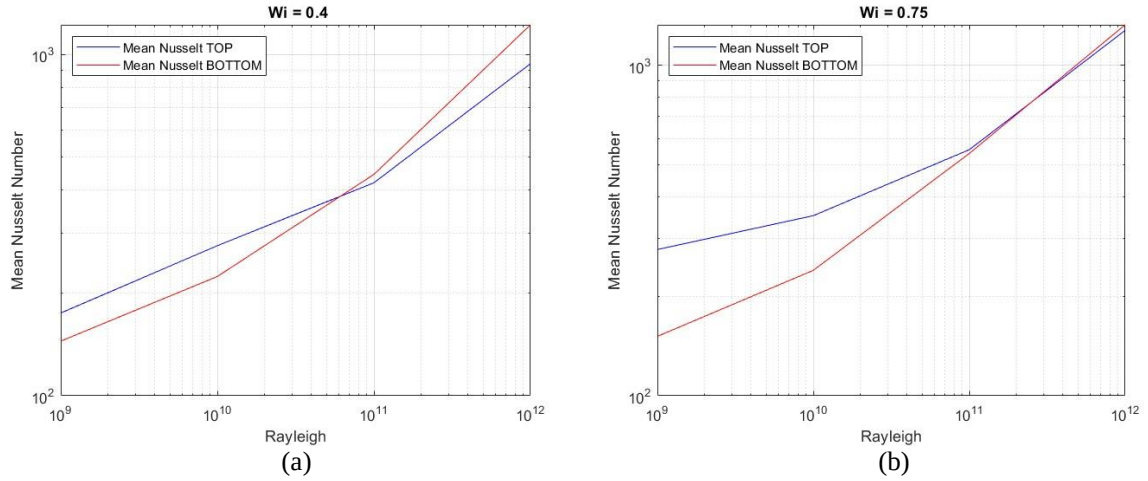

Figure 5. Variation of mean top and mean bottom Nusselt number with Rayleigh number for the case where (a) W_i = 0.4 and (b) W_i = 0.75.

Table 1. Simulation and calculated results were obtained for one adiabatic section.

	W_i = 0.1				W_i = 0.2			
Ra_L	$q_{(top)}$ [W]	$q_{(bottom)}$ [W]	$Nu_{L(top)}$	$Nu_{L(bottom)}$	$q_{(top)}$ [W]	$q_{(bottom)}$ [W]	$Nu_{L(top)}$	$Nu_{L(bottom)}$
1.10^9	54.2566	77.7448	124.5560	178.4776	54.6714	55.3922	141.1969	143.0585
1.10^{10}	93.1683	94.5527	213.8850	217.0631	90.3901	85.0337	233.4455	219.6118
1.10^{11}	124.4347	201.1801	285.6628	461.8458	146.1117	175.1026	377.3547	452.2277
1.10^{12}	320.6061	613.8247	736.0103	1,409.1476	312.7214	438.3054	807.6483	1131.9871
	W_i = 0.4				W_i = 0.75			
Ra_L	$q_{(top)}$ [W]	$q_{(bottom)}$ [W]	$Nu_{L(top)}$	$Nu_{L(bottom)}$	$q_{(top)}$ [W]	$q_{(bottom)}$ [W]	$Nu_{L(top)}$	$Nu_{L(bottom)}$
1.10^9	50.7476	41.9702	174.7507	144.5257	33.5329	18.3053	277.1313	151.2832
1.10^{10}	79.9277	64.9273	275.2330	223.5788	42.4591	29.0082	350.9017	239.7370
1.10^{11}	122.1741	129.2948	420.7095	445.2301	67.2442	65.5038	555.7369	541.3537
1.10^{12}	272.9377	354.7836	939.8679	1221.7067	154.5009	160.6363	1276.8672	1327.5726

For two adiabatic sections, the simulation was realized for the width of the adiabatic sections ranging from 0.05, 0.1, 0.2, and 0.375 m. These results can be seen in Fig. 6 and 7.

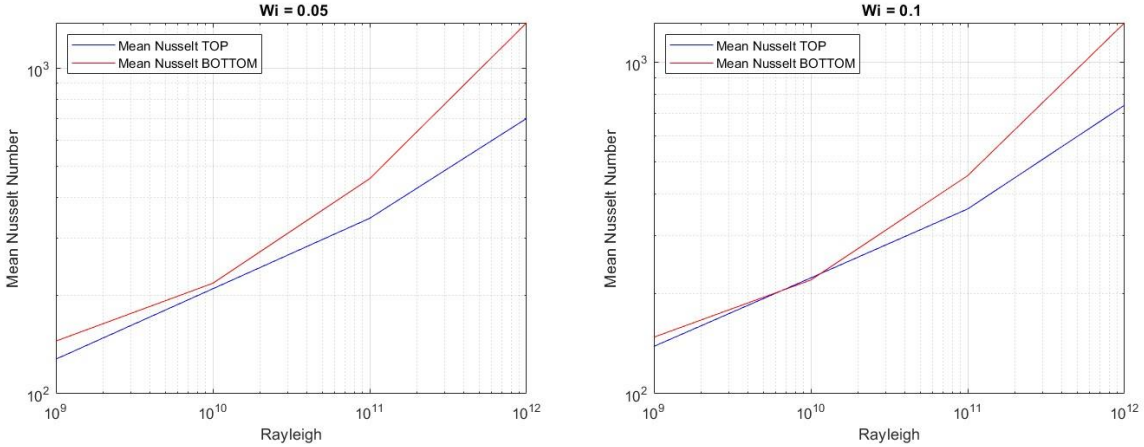

(a) (b)

Figure 6. Variation of mean top and mean bottom Nusselt number with Rayleigh number for the case where (a) W_i = 0.05 and (b) W_i = 0.1.

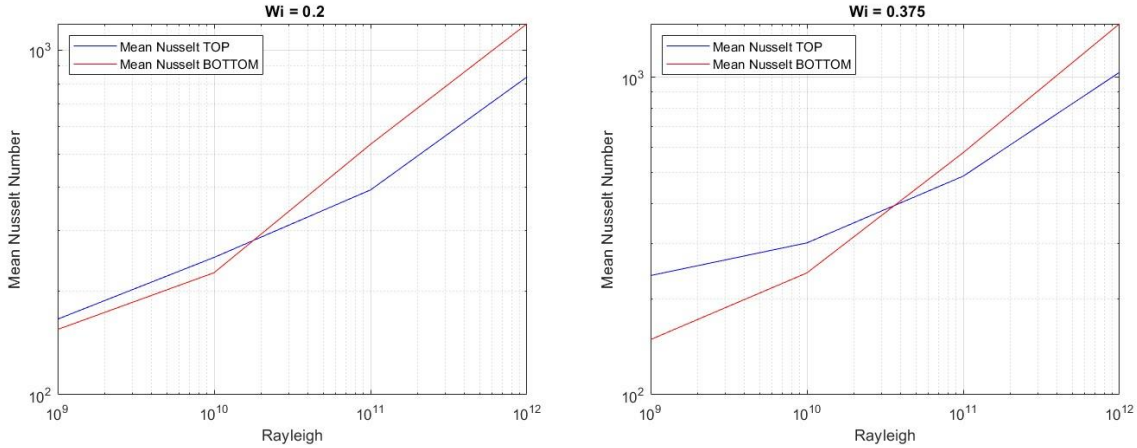

(a) (b)

Figure 7. Variation of mean top and mean bottom Nusselt number with Rayleigh number for the case where (a) W_i = 0.2 and (b) W_i = 0.375.

The Tab. 2 contains these results in terms of Nusselt number and heat transfer rate for the top and the bottom regions for each respective Rayleigh number.

Table 2. Simulation and calculated results were obtained for two adiabatic sections.

	Wi = 0.05				Wi = 0.1			
Ra_L	$q_{(top)}$ [W]	$q_{(bottom)}$ [W]	$Nu_{L(top)}$	$Nu_{L(bottom)}$	$q_{(top)}$ [W]	$q_{(bottom)}$ [W]	$Nu_{L(top)}$	$Nu_{L(bottom)}$
1.10^9	55.6294	63.2217	127.7075	145.1370	53.8069	57.3622	138.9640	148.1462
1.10^{10}	91.5451	95.1731	210.1585	218.4874	86.5949	85.3182	223.6439	220.3467
1.10^{11}	150.7555	199.5650	346.0869	458.1382	139.8751	176.2860	361.2477	455.2842
1.10^{12}	305.5668	601.1694	701.4848	1380.0951	287.6982	509.9114	743.0222	1316.9198
	Wi = 0.2				Wi = 0.375			
Ra_L	$q_{(top)}$ [W]	$q_{(bottom)}$ [W]	$Nu_{L(top)}$	$Nu_{L(bottom)}$	$q_{(top)}$ [W]	$q_{(bottom)}$ [W]	$Nu_{L(top)}$	$Nu_{L(bottom)}$
1.10^9	48.1315	44.9249	165.7420	154.7000	28.7162	18.0530	237.3237	149.1983
1.10^{10}	72.7191	65.6482	250.4100	226.0615	36.3886	29.2677	300.7323	241.8821
1.10^{11}	114.1555	154.8449	393.0973	533.2124	59.0326	70.0149	487.8725	578.6355
1.10^{12}	242.8767	346.5004	836.3523	1193.1832	125.3270	178.1532	1035.7601	1472.3407

The results obtained to flat plate without adiabatic sections for Rayleigh number varying between 10^9 to 10^{12} could be seen in Fig. 8.

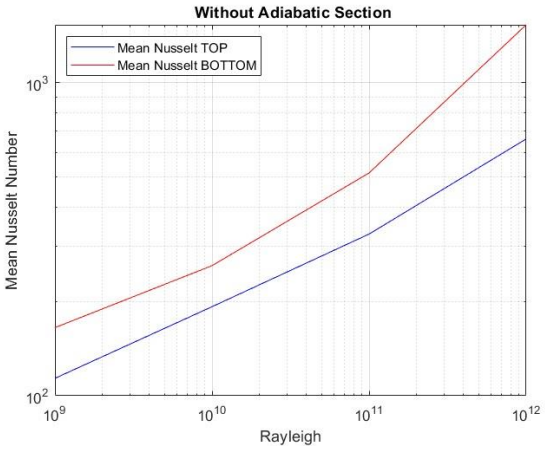

(a)

Ra_L	$q_{(top)}$ [W]	$q_{(bottom)}$ [W]	$Nu_{L(top)}$	$Nu_{L(bottom)}$
1.10^9	55.0245	79.9087	113.6869	165.1006
1.10^{10}	93.2016	126.0566	192.5653	260.4475
1.10^{11}	159.0817	249.4419	328.6812	515.3759
1.10^{12}	320.2740	741.9810	661.7231	1533.0186

(b)

Figure 8. (a) Variation of mean top and mean bottom Nusselt number with Rayleigh number for the case where without adiabatic section and (b) simulation results obtained for flat plate without adiabatic sections.

To compare the performance between heat transfer with and without adiabatic section, variations of the mean top (a) and the mean bottom (b) Nusselt number with the Rayleigh number and for values of *W*i varying between 0.1 and 0.75 for the case with one adiabatic section in Fig. 9 to 12.

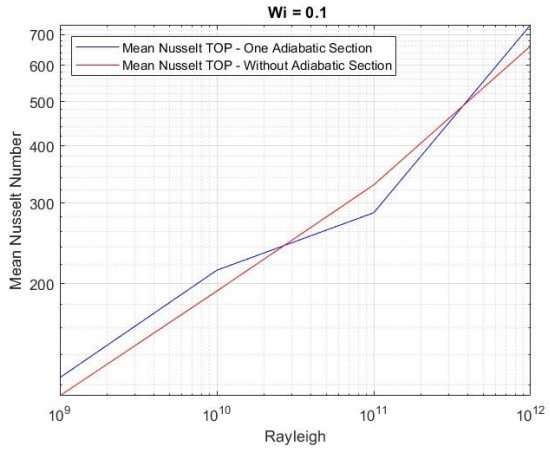

(a)

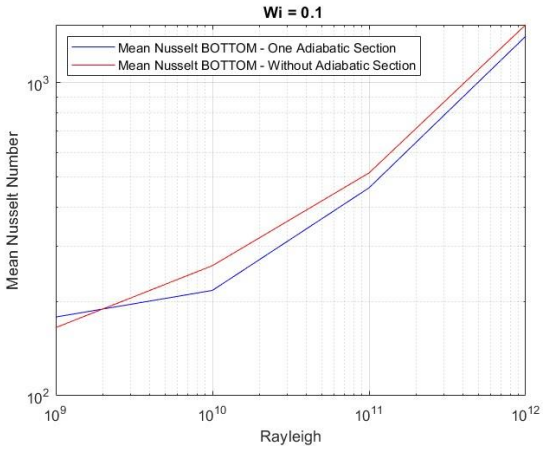

(b)

Figure 9. Variation of the mean top (a) and mean bottom (b) Nusselt number between one adiabatic section with W_i = 0.1 and the case without adiabatic section for the same Rayleigh number.

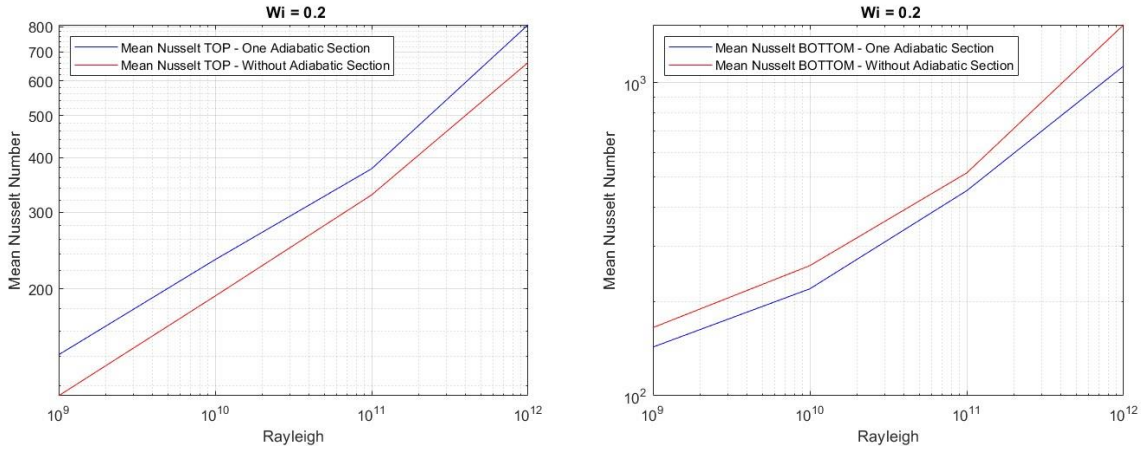

(a) (b)

Figure 10. Variation of the mean top (a) and mean bottom (b) Nusselt number between one adiabatic section with W_i = 0.2 and the case without adiabatic section for the same Rayleigh number.

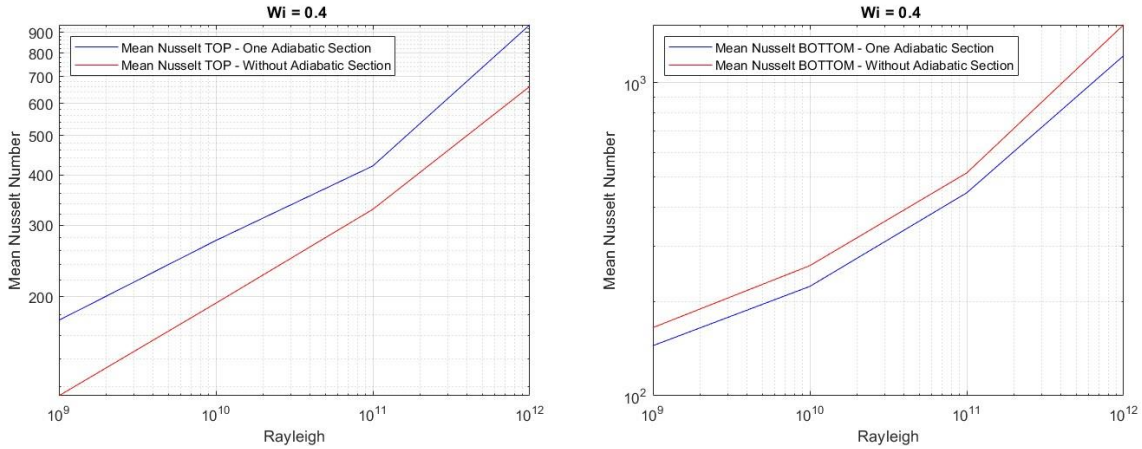

(a) (b)

Figure 11. Variation of the mean top (a) and mean bottom (b) Nusselt number between one adiabatic section with W_i = 0.4 and the case without adiabatic section for the same Rayleigh number.

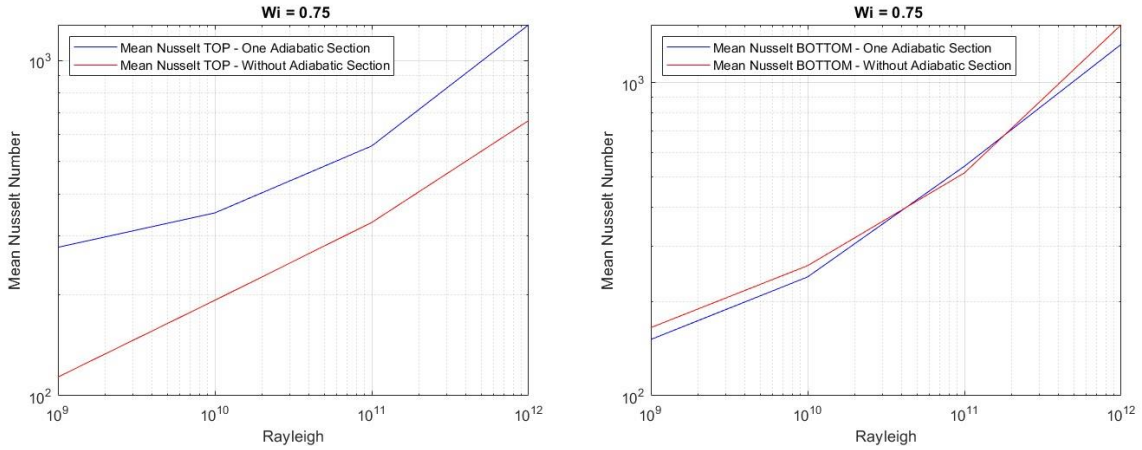

(a) (b)

Figure 12. Variation of the mean top (a) and mean bottom (b) Nusselt number between one adiabatic section with W_i = 0.75 and the case without adiabatic section for the same Rayleigh number.

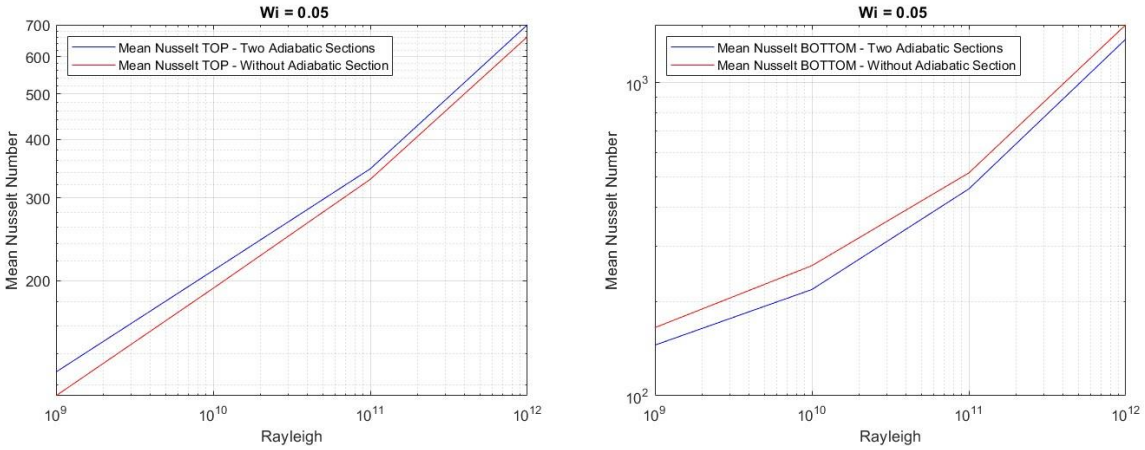

(a) (b)

Figure 13. Variation of the mean top (a) and mean bottom (b) Nusselt number between two adiabatic sections with W_i = 0.05 and the case without adiabatic section for the same Rayleigh number.

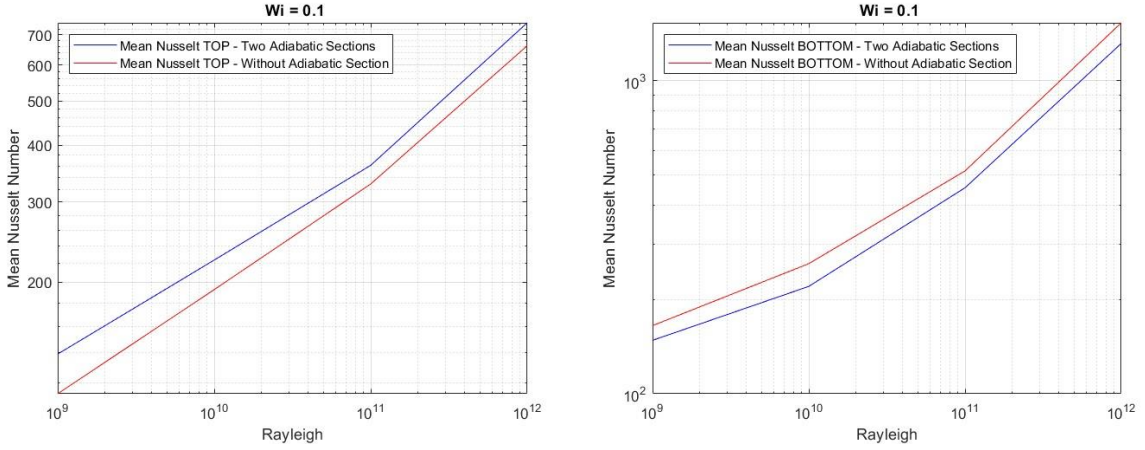

(a) (b)

Figure 14. Variation of the mean top (a) and mean bottom (b) Nusselt number between two adiabatic sections with W_i = 0.1 and the case without adiabatic section for the same Rayleigh number.

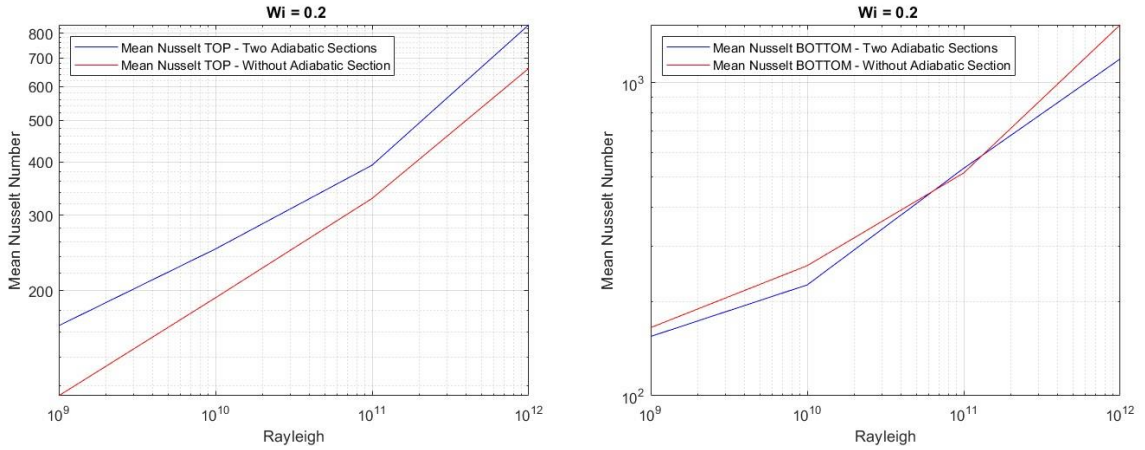

(a) (b)

Figure 15. Variation of the mean top (a) and mean bottom (b) Nusselt number between two adiabatic sections with W_i = 0.2 and the case without adiabatic section for the same Rayleigh number.

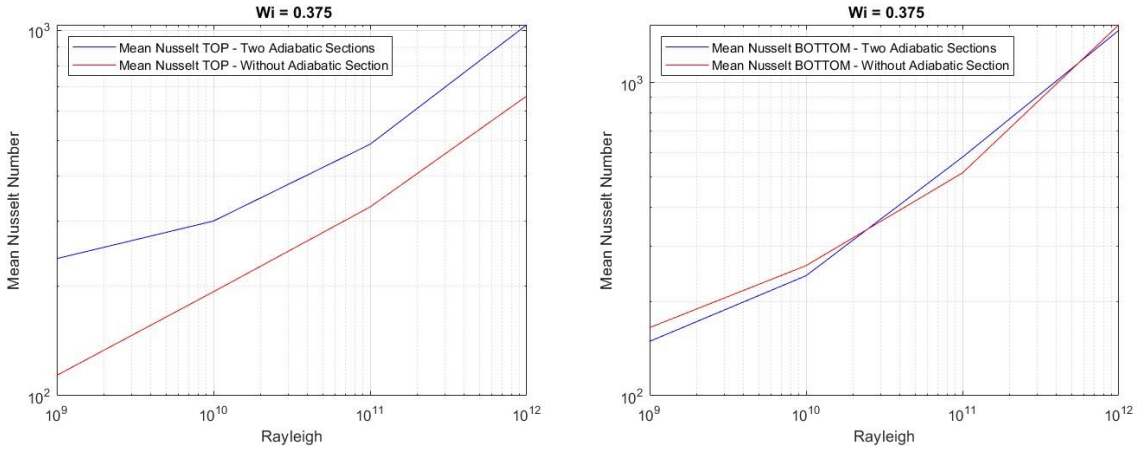

Figure 16. Variation of the mean top (a) and mean bottom (b) Nusselt number between two adiabatic sections with W_i = 0.375 and the case without adiabatic section for the same Rayleigh number.

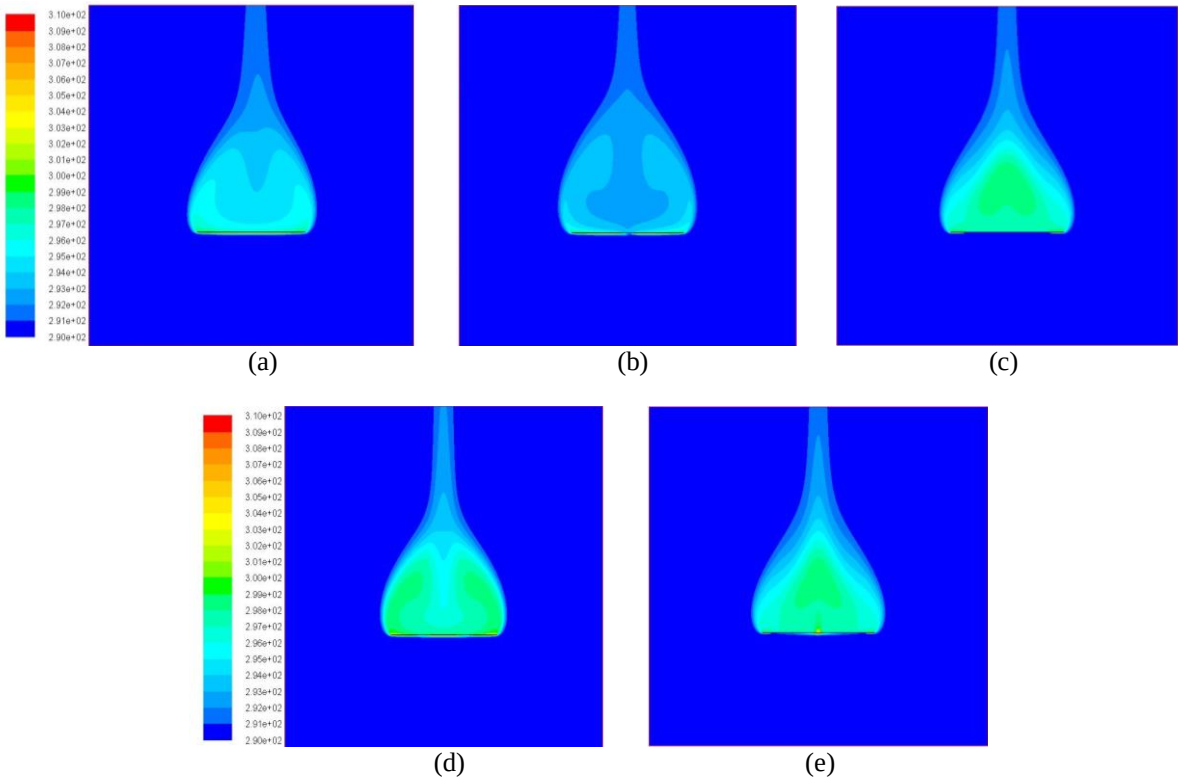

Figure 17. Temperature distribution for 10^9 Rayleigh for cases (a) flat plate without adiabatic section (b) one adiabatic section with W_i = 0.1, (c) one adiabatic section with W_i = 0.75, (d) two adiabatic sections with W_i = 0.1 and (e) two adiabatic sections with W_i = 0.375.

5. CONCLUSIONS

According to Fig. 4 and 5, it was possible to verify that, with only one adiabatic section, the Nusselt number top section was higher for low Rayleigh numbers in the cases where W_i = 0.4 and 0.75, while for higher Rayleigh numbers, the bottom Nusselt number was higher in all cases. For two adiabatic sections, the results obtained in Fig. 6 and 7 showed the same behavior where, for larger sections (W_i = 0.2 and 0.375) the top Nusselt number started higher for lower Rayleigh numbers, while for taller Rayleigh the Nusselt number was higher for the bottom section in all cases.

Figure 8 showed that for the flat plate without adiabatic sections, the heat transfer occurs more strongly in the bottom section of the plate. In order to compare the performance between heat transfer with and without adiabatic section, variations of the mean top (a) and the mean bottom (b) presents in Fig. 9 to 16 made these possible. In

practically all the cases (with one or two adiabatic sections) the top region (a) with adiabatic section presented a better performance in terms of mean Nusselt number compared to the same plate without adiabatic section, while for the bottom section (b) the opposite was verified, where the adiabatic sections reduced the mean Nusselt Number compared to plate without adiabatic sections, where for only some Rayleigh points the adiabatic section performance was better, as in the case of Fig. 16 (b) for 10^{11} Rayleigh. So, knowing how the adiabatic sections interfere in the heat transfer, the configurations with adiabatic sections are more indicated when wants to intensify the heat transfer relation in the bottom region, where the highest relation was realized for one adiabatic section with 10^9 Rayleigh and W_i=0.75.

Figure 17 showed the behavior of the model for the temperature distribution, being possible to verify how the adiabatic sections influence the flow and the heat transfer compared to the plate without adiabatic sections. The heat transfer in the top section has similar values for all the cases, while the bottom section has a bigger difference compared to the plate without adiabatic section. It is also possible to verify that the larger the adiabatic section (one or two) the greater your influence on temperature.

6. REFERENCES

Adhikari, R. C., Wood, D. H., and Pahlevani, M., 2020. "Optimizing rectangular fins for natural convection cooling using CFD." Thermal Science and Engineering Progress, Vol. 17, pp. 100484.

Çengel, Y. A., and Ghajar, A. J., 2009. Transferência de Calor e Massa. AMGH editora.

Dogan, M., Sivrioglu, M., and Yılmaz, O., 2014. "Numerical analysis of natural convection and radiation heat transfer from various shaped thin fin-arrays placed on a horizontal plate-a conjugate analysis." Energy conversion and management, Vol. 77, pp. 78-88.

Fayz-Al-Asad, M., Alam, M. N., Rashad, A. M., and Sarker, M. M. A., 2021. "Impact of undulation on magneto-free convective heat transport in an enclosure having vertical wavy sides". International Communications in Heat and Mass Transfer, Vol. 127, pp. 105579.

Guha, A., Jain, A., and Pradhan, K., 2019. "Computation and physical explanation of the thermo-fluid-dynamics of natural convection around heated inclined plates with inclination varying from horizontal to vertical". *International Journal of Heat and Mass Transfer*, Vol. 135, pp. 1130-1151.

Hærvig, J., and Sørensen, H., 2020. "Natural convective flow and heat transfer on unconfined isothermal zigzag-shaped ribbed vertical surfaces". *International Communications in Heat and Mass Transfer*, Vol. 119, pp. 104982.

Incropera, F. P., and DeWitt, D. P., 2008. *Fundamentos de transferência de calor*. LTC.

Jiji, L. M., and Jiji, L. M., 2006. *Heat convection*. Berlin: Springer.

Kitamura, K., and Kimura, F., 1995. "Heat transfer and fluid flow of natural convection adjacent to upward-facing horizontal plates". *International journal of heat and mass transfer*, Vol. 38, No. 17, pp. 3149-3159.

Laein, R. P., Rashidi, S., and Esfahani, J. A., 2016. "Experimental investigation of nanofluid free convection over the vertical and horizontal flat plates with uniform heat flux by PIV". *Advanced Powder Technology*, Vol. 27, No. 2, pp. 312-322.

Liu, L., Chen, W., Wang, C., and Hu, C., 2021. "CFD analysis of steam condensation with air in the tubes bundle channel under natural convection conditions". Annals of Nuclear Energy, Vol. 162, pp. 108510.

Narayana, P. L., and Sibanda, P., 2010. "Soret and Dufour effects on free convection along a vertical wavy surface in a fluid saturated Darcy porous medium". *International Journal of Heat and Mass Transfer*, Vol. 53, No. 15-16, pp. 3030-3034.

Nazar, R., Arifin, N. M., and Pop, I., 2006. "Free convection boundary layer flow over vertical and horizontal flat plates embedded in a porous medium under mixed thermal boundary conditions". *International communications in heat and mass transfer*, Vol. 33, No. 1, pp. 87-93.

Samanta, S., and Guha, A., 2014. "Analysis of heat transfer and stability of magnetohydrodynamic natural convection above a horizontal plate with heat flux boundary condition". *International Journal of Heat and Mass Transfer*, Vol. 70, pp. 793-802.

SV, S. S. S., Ranganath, R., Shaju, S., Seetharam, T. R., and Seetharamu, K. N., 2021. "Numerical predictions of forced convection and free convection heat transfer from an isothermal horizontal flat plate to supercritical nitrogen". *Thermal Science and Engineering Progress*, Vol. 23, pp. 100867.

Tari, I., and Mehrtash, M., 2013. "Natural convection heat transfer from horizontal and slightly inclined plate-fin heat sinks". *Applied Thermal Engineering*, Vol. 61, No. 2, pp. 728-736.

Versteeg, H. K., and Malalasekera, W., 2007. *Computational fluid dynamics. The finite volume method*. Pearson Educatoin Limited, 2nd edition.

Yu, W. S., and Lin, H. T., 1993. "Conjugate problems of conduction and free convection on vertical and horizontal flat plates". *International journal of heat and mass transfer*, Vol. 36, No. 5, pp. 1303-1313.

7. RESPONSIBILITY NOTICE

The authors are the only responsible for the printed material included in this paper.